Science of the Total Environment 760 (2021) 143235

Contents lists available at ScienceDirect

Science of the Total Environment

journal homepage: www.elsevier.com/locate/scitotenv

The effects of antimony on Alzheimer's disease-like pathological changes in mice brain

Shenya Xu [a,1], Zeyun Yang [b,1], Ye Zhi [a], Shali Yu [a], Tao Zhang [a], Junkang Jiang [a], Jun Tang [c], Hongsen He [c], Ming Lu [d,e,f], Xiaoke Wang [a,*], Qiyun Wu [a,f,**], Xinyuan Zhao [a,*]

[a] Department of Occupational Medicine and Environmental Toxicology, School of Public Health, Nantong University, Nantong 226019, China
[b] Nantong Center for Disease Control and Prevention, Nantong 226007, China
[c] Zhejiang Provincial Center for Disease Control and Prevention, Hangzhou, China
[d] Clinical Epidemiology Unit, Qilu Hospital of Shandong University, Jinan, China
[e] Clinical Research Center of Shandong University, Jinan, China
[f] Fudan University Taizhou Institute of Health Sciences, Taizhou, China

HIGHLIGHTS

- Antimony (Sb) promoted β-amyloid protein (Aβ) accumulation at mice brain treated for 4 weeks.
- Sb increased tau phosphorylation at ser396 and ser199, and number of neurofibrillary tangles (NFTs) for 8 weeks and 1 year.
- Our findings directly prove that Sb is a novel nerve poison possessing AD risk.

GRAPHICAL ABSTRACT

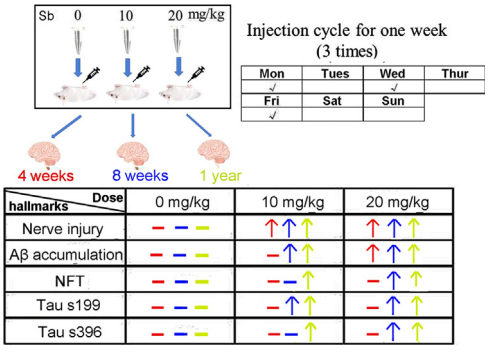

ARTICLE INFO

Article history:
Received 19 July 2020
Received in revised form 3 October 2020
Accepted 4 October 2020
Available online 26 October 2020

Editor: Henner Hollert

Keywords:
Antimony
Neurotoxicity
Alzheimer's disease
Aβ accumulation
Tau phosphorylation

ABSTRACT

We have previously identified antimony (Sb) as a newly nerve poison which leads to neuronal apoptosis. However, the relationship between Sb exposure and Alzheimer's disease (AD) process lacks direct evidence. HE staining and Nissl staining showed significant nerve damage after Sb exposure. Therefore, we further evaluated Sb-associated AD risk by detecting accumulation of β-amyloid protein (Aβ) and neurofibrillary tangles (NFTs) in the brains of mice exposed to Sb for 4 and 8 weeks, and even 1 year. The results showed that dose of 20 mg/kg induced Aβ accumulation, but not tau hyperphosphorylation after exposure for 4 week. Eight weeks later, both 10 and 20 mg/kg dramatically triggered Aβ accumulation and increased tau phosphorylation at ser199. At the same time, 20 mg/kg could also increase tau phosphorylation at ser396 and number of NFTs. One years later, we found all of AD hallmarks detected in present study showed positive results in the brains of mice exposed to Sb at 10 and 20 mg/kg. In summary, our data provided direct evidence of Sb-associated AD risk, drawing more attention to Sb-triggered neurotoxicity.

1. Introduction

Alzheimer's disease (AD) is a neurodegenerative condition characterised primarily by impaired cognition and memory, and dementia (Liu et al., 2019). A recent systematic meta-analysis found

* Corresponding authors.
** Correspondence to: Q. Wu, Fudan University Taizhou Institute of Health Sciences, Taizhou, China.
E-mail addresses: wxk11628@ntu.edu.cn (X. Wang), wqy@ntu.edu.cn (Q. Wu), zhaoxinyuan@ntu.edu.cn (X. Zhao).
[1] These authors contributed equally to this work.

https://doi.org/10.1016/j.scitotenv.2020.143235
0048-9697/

that over 50 million people worldwide have dementia (principally AD). In the United States, AD has become the fifth leading cause of death among those aged over 65 years. In 2018, AD deaths in the United States numbered 122,019; both morbidity and mortality are increasing (2020). The aetiology of AD remains unclear, although the amyloid cascade, tau, and cholinergic (principally the former two) hypotheses have attracted much attention. Amyloid plaques formed via accumulation of β-amyloid protein (Aβ) outside the cell and neurofibrillary tangles (NFTs) created via overphosphorylation of the tau protein are the two most important pathological features of AD brains (Li et al., 2018). Aβ accumulation induces neuronal dysfunction via various mechanisms including synaptic damage and abnormal axonal conduction, and damages organelles including the mitochondrion and Golgi apparatus (Arbel-Ornath et al., 2017; Choi et al., 2017; Joshi et al., 2014; Volgyi et al., 2015). Tau overphosphorylation compromises microtubule stability, inducing synaptic dysfunction (Hoover et al., 2010).

The known AD risk factors are both environmental and genetic. About 0.1% of all AD reflects autosomal dominant inheritance (familial AD) (Blennow et al., 2006). However, the vast majority of AD cases (sporadic AD) lack this feature (Strittmatter et al., 1993). Exposure to environmental pollutants has become a major risk factor for multiple diseases, including AD. Many epidemiological and toxicological studies have shown that metal pollutants affect the cognitive abilities of humans and animals, and play important roles in AD pathogenesis (Liu et al., 2019). Aluminium exposure promotes AD, as confirmed in many studies (Oshima et al., 2013). Elevated blood cadmium levels in AD patients over 60 years of age increase mortality (Min and Min, 2016). Other metals (lead, manganese, and arsenic) also promote AD (Huat et al., 2019). For example, lead significantly increases the expression of mouse amyloid precursor (APP) and thus Aβ synthesis (Zhou et al., 2018). Manganese induces tau hyperphosphorylation in vitro (Cai et al., 2011). Moreover, lead, arsenic, and cadmium synergistically increase Aβ expression in the mouse brain (Ashok et al., 2015). Are other metals associated with AD development?

Antimony (Sb) is a metal found in soil, drinking water, and foodstuffs. Non-occupationally exposed people exhibit low long-term Sb intake (Sundar and Chakravarty, 2010). However, some industrial activities (such as the mining and smelting of Sb ore) are associated with the release of large amounts of Sb into natural environments. Workers in these fields live in environments with high concentrations of Sb (Saerens et al., 2019). In cities, automobile exhaust is an important source of Sb pollution (Long et al., 2020). Long-term Sb exposure seriously compromises respiratory and cardiovascular function (Sundar and Chakravarty, 2010). Sb accumulates in the human and mouse brain, encouraging researchers to explore Sb-associated neurotoxicity. Recently, Tanu et al. found that that intraperitoneal Sb injection impaired mouse cognitive function in the Morris water maze test, indicating that Sb pollution might be associated with a risk of AD (Tanu et al., 2018). Later, we reported that protein kinase B (Akt) inhibition played a critical role in Sb-mediated neuronal apoptosis by triggering mammalian target of rapamycin (mTOR) inhibition-dependent autophagy and suppressing Wnt/β-catenin signalling (Shi et al., 2020; Wang et al., 2019). As neuronal cell death is a prominent feature of AD, we concluded that Sb was a novel nerve poison and a potential AD risk factor.

However, experimental data about the effects of Sb on AD hallmarks are lacking. Here, we assessed pathological AD features in the mice brain exposed to Sb. The aim of our study was to provide direct evidence to support Sb was a risk factor for AD; thus, draw more attention to Sb-triggered neurotoxicity.

2. Materials and methods

2.1. Reagents and antibodies

We purchased potassium antimonyl tartrate trihydrate (Sigma, 60063), anti-Aβ antibody (Proteintech, 25524-1-AP), anti-tau antibody (Proteintech, 10274-1-AP), anti-ACTB antibody (Santa Cruz, sc-47778), anti-tau [ser199] antibody (abcam, ab81268), and anti-tau [ser396] antibody (abcam, ab109390).

2.2. Animals

Ninety 6-week-old ICR male mice (25–30 g) were purchased from the Experimental Animal Center of Nantong University. All animal experiments were approved by the Experimental Animal Ethics Committee of Nantong University. The mice were housed under a 12-/12-h dark/light cycle with free access to drinking water and food. After 1 week of adaptive feeding, all mice were randomly divided into groups receiving 0, 10, and 20 mg/kg of intraperitoneal Sb (three times weekly) for 4 and 8 weeks, we also exposed mice to Sb for 1 year (intraperitoneal injection for 44 weeks and drawing off exposure for 8 weeks to mimic work and retirement). It should be noted that the doses used in present study were comparable to that of human beings. In detail, as reported in previous publication (Tanu et al., 2018), the Sb concentration in mice brain under current experimental conditions was 4.66 ± 0.076 ng/g. Moreover, the Sb concentration in human brain was about 2.5–170.7 × 10^{-6} g/g (Hock et al., 1975), which was higher than present mice model. In addition, the dose administered intravenously to humans over alternate days reached by 2.5 g (about 40 mg/kg) to treat schistosomiasis (Dieter et al., 1991). Therefore, we believe that Sb possessed neurotoxicity under an accessible dose. The control groups (0 mg/kg) were injected with 100 μL of 0.9% (w/v) saline. The Sb-exposed groups were injected with 100 μL of the Sb solutions. After 4 and 8 weeks and 1 year, one third of mice in each group were randomly sacrificed and the brains removed. A small piece of brain tissue was fixed in 4% (v/v) paraformaldehyde for histological analysis and the remaining tissue stored at −80 °C.

2.3. Haematoxylin and eosin (HE) and Nissl staining

Fixed mouse brain tissue was embedded in paraffin and sectioned (thickness 5 μm). The sections were placed in xylene, and then ethanol (for dewaxing and rehydration). HE staining proceeded as instructed by the kit manufacturer (Beyotime, C0105). After staining with haematoxylin for 10 min, excess solution was washed away with water. The slides were immersed in 5% (v/v) glacial acetic acid/alcohol for 40 s, rinsed with water, stained with eosin for 2 min, dehydrated with ethanol and xylene, and observed after mounting.

After initial dewaxing and rehydration, Nissl staining proceeded as instructed by the kit manufacturer (Beyotime, C0117). After staining with Nessler's solution for 10 min, the slides were quickly washed twice with water for several seconds each time. After immersing the slides in 95% ethanol for several seconds, they were dehydrated with ethanol and xylene and mounted for observation.

2.4. Western blotting

Brain tissue (cerebral cortex) was added to protein lysis buffer and rapidly homogenised and centrifuged. The supernatant protein concentration was determined using a bicinchoninic acid protein assay kit (Beyotime, P0009). Equal amounts of protein (50 μg per sample) were

Fig. 1. Antimony exposure causes brain damage in mice. (a) Histopathological images of HE-stained Sb-exposed mouse brains at indicated doses (0, 10, 20 mg/kg) and duration (4 weeks, 8 weeks, one year). (b) Nissl-stained histopathological images of mouse brains treated as (a). Scale bar: 50 μm. n = 3.

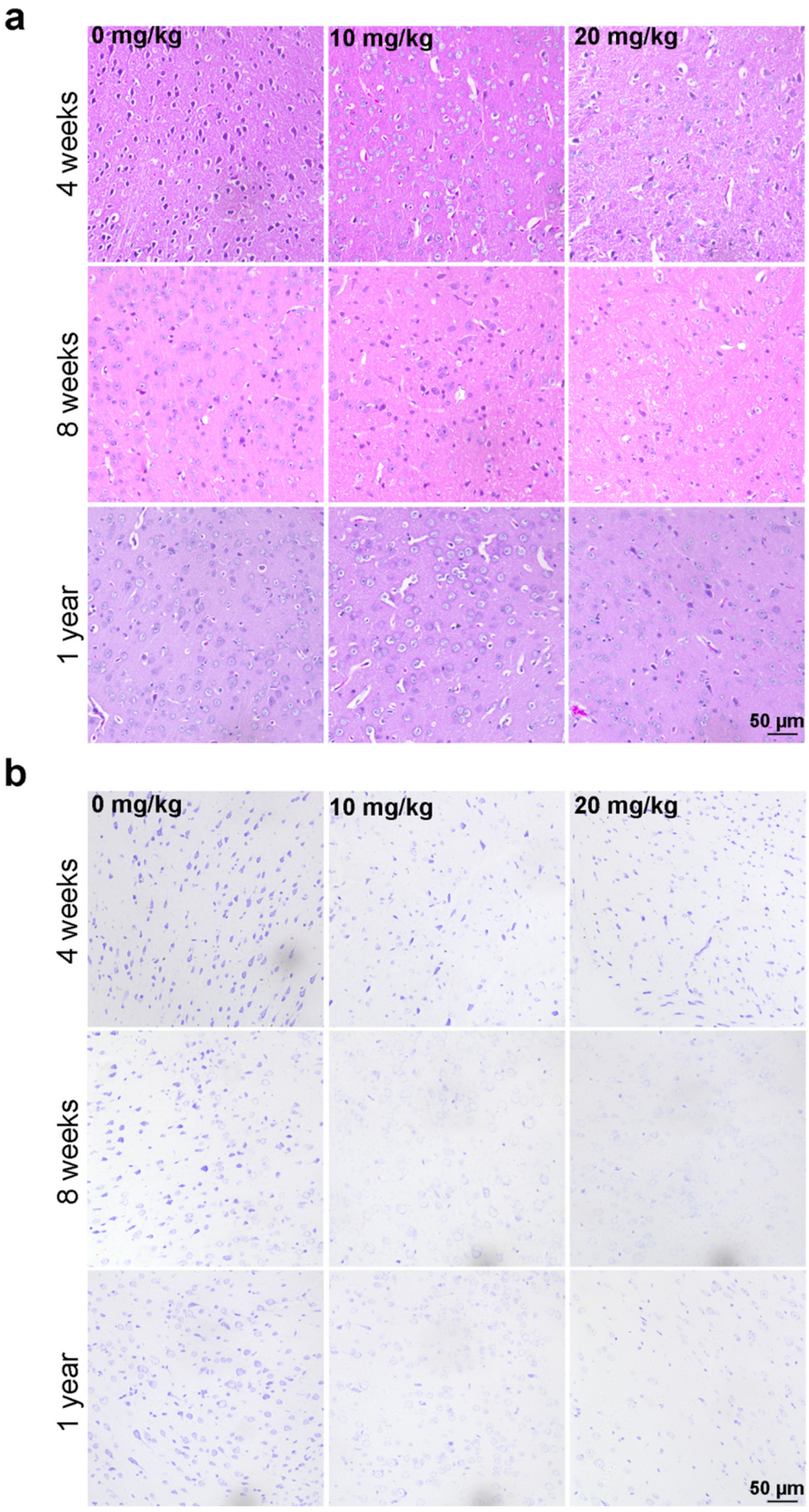
a
0 mg/kg
10 mg/kg
20 mg/kg
4 weeks
8 weeks
1 year
50 μm
b
0 mg/kg
10 mg/kg
20 mg/kg
4 weeks
8 weeks
1 year
50 μm

separated via sodium dodecyl sulphate polyacrylamide gel electrophoresis and transferred to polyvinylidene fluoride membranes. The membranes were incubated in buffer with 3% (w/v) bovine serum albumin (BSA) for 2 h, the primary antibodies (anti-Aβ, 1:1000; anti-tau, 1:1000; anti-tau [ser199], 1:1000; anti-tau [ser396], 1:1000; and anti-ACTB, 1:2000) were added, which was followed by overnight incubation at 4 °C and incubation with goat anti-mouse or anti-rabbit IgG secondary antibody coupled with horseradish peroxidase for 1 h. Finally, an enhanced chemiluminescence kit (Millipore, P90720) was used to observe protein bands.

2.5. Immunohistochemistry

Brain tissue paraffin sections were dewaxed in xylene and rehydrated in ethanol. The slides were immersed in a 10% (w/v) sodium citrate solution at 95 °C for 30 min (antigen retrieval) and then cooled to room temperature. Endogenous peroxidase activity was blocked with 3% (v/v) hydrogen peroxide and BSA added to 3% (w/v) followed by incubation at room temperature for 2 h. Brain tissues were next incubated with primary antibodies (anti-Aβ, 1: 300; anti-tau, 1: 200; anti-tau [ser199], 1: 250; and anti-tau [ser396], 1: 500) at 4 °C overnight; the secondary antibodies (1: 1000) were then added for incubation for 1 h. The sections were dehydrated after colour development with 3,3′-diaminobenzidine and counterstaining with haematoxylin. Finally, protein expression was observed under a microscope (Leica Microsystems).

2.6. Bielschowsky staining

After mouse brain slices were dewaxed in xylene and ethanol and rehydrated, the following steps were performed as recommended by the kit manufacturer (Solarbio, G3260). After washing the slides, they were immersed in the Bielschowsky silver solution and placed in a 37 °C incubator for 40 min in the dark. After washing with distilled water, the tissue was reduced (becoming yellow) with a reducing agent. After washing again with water and staining with ammonia-silver solution for 40 s, the staining solution was poured away and the tissue repeatedly browned with a reducing agent. After washing with water for 5 min, the tissue was stained with Hypo solution for 10 min. Finally, after washing with water for 2 min, gold chloride solution was added for 5 min. After dehydration with ethanol and xylene, the slides were mounted and observed.

2.7. Statistical analysis

All data are presented as means ± standard deviations. We used Student's *t*-test or one way ANOVA analysis to compare the groups. All statistical analyses were performed with the aid of GraphPad Prism ver. 7.0. A p-value < 0.05 was taken to indicate statistical significance.

3. Results

3.1. Sb causes nerve damage

To evaluate the effect of Sb on the mouse brain, we performed HE and Nissl staining. HE staining revealed that the neurons of control brains were closely packed, the cell bodies round, and the nuclei obvious. Sb-exposed brains exhibited nuclear loss and shrinkage, and cellular atrophy (Fig. 1a). These pathological effects increased over time (Fig. 1a). Nissl staining revealed a similar trend. As the Sb dose rose and the exposure time increased, the number of Nissl bodies gradually decreased (Fig. 1b). Collectively, the data suggest that Sb causes nerve damage in a dose- and time-dependent manner.

3.2. Sb induces Aβ accumulation in mouse brain

Aβ accumulation is a major pathological feature during AD progression. We measured Aβ levels via Western blotting. Sb at 10 mg/kg dramatically increased the Aβ expression levels at 8 weeks and 1 year, but not at 4 weeks. However, Sb at 20 mg/kg significantly increased Aβ expression levels at all three timepoints (Fig. 2a, b, and c). Immunohistochemistry yielded similar results (Fig. 2d). Notably, the Aβ expression levels in control brains also increased over time, supporting the idea that aging is a risk factor for AD development (Fig. 2d). Together, the results show that Sb triggers accumulation of Aβ plaques in the mouse brain; this is evidence of an Sb-associated AD risk.

3.3. Sb increases the numbers of NFTs in mouse brain

We used Bielschowsky staining to explore morphological and quantitative changes in NFT numbers, another major pathological feature of AD, during Sb exposure. At 4 weeks, the neurons in the cerebral cortices of the control and Sb (10 mg/kg)-exposed mice were loosely arranged, and the cells were round and light in colour with no tailing; the axons stained dark. However, in the Sb (20 mg/kg)-exposed group, the neuronal cell bodies were dark with thick, heavily stained tails (Fig. 3). At 8 weeks, both the control and Sb (10 mg/kg)-exposed group were stained as at 4 weeks. In the Sb (20 mg/kg)-exposed group, small numbers of NFTs were clearly observed (Fig. 3). At 1 year, as expected, NFTs were observed in the brains of all Sb-exposed mice, and the numbers of neurons that were morphologically normal were significantly reduced; the largest number of NFTs was observed in the Sb (20 mg/kg)-exposed group (Fig. 3).

3.4. Effects of Sb on tau phosphorylation at ser396 and ser199

Tau hyperphosphorylation is the principal cause of NFT formation. We measured tau phosphorylation at ser199 and ser396 via Western blotting. The total tau levels were identical in all groups at all timepoints (Fig. 4a, b, c). Although abnormal changes in neuronal morphology were evident in the brains of mice exposed to Sb at 20 mg/kg for 4 weeks, no significant upregulation of tau phosphorylation at ser199 or ser396 was apparent (Fig. 4a). However, both residues were hyperphosphorylated at ser199 in mice exposed to 10 and 20 mg/kg Sb for 8 weeks or 1 year (Fig. 4b, c). Ser396 phosphorylation was not affected by exposure to 10 mg/kg Sb for 8 weeks, but was dramatically upregulated at 1 year. Sb at 20 mg/kg increased ser396 phosphorylation after 8 weeks and 1 year (Fig. 4b, c). Immunochemistry confirmed these results (Fig. 5a, b, c). We found a gradual increase in tau phosphorylation with aging of the control group (Fig. 5). In conclusion, Sb stimulated NFT accumulation and tau hyperphosphorylation.

4. Discussion

With the amyloid and tau protein hypotheses of AD pathogenesis in mind, we evaluated the Sb-associated AD risk, and found that Sb caused Aβ accumulation and tau hyperphosphorylation in the mouse brain, suggesting that Sb possesses AD risk.

Aβ deposits from an imbalance between production and clearance of Aβ peptides is an early, often initiating factor in AD (Selkoe and Hardy, 2016). Aβ derives from the amyloid precursor protein (APP), a large type I transmembrane protein, followed by its cleavage by enzymes termed β- and γ-secretase (Ehehalt et al., 2003). Although we did not explore molecular mechanisms underlying Aβ accumulation in present study, several previous publications from our group provided potential clues to possible mechanism. Recently, we reported that Sb activated GSK3β and subsequently inhibited the Wnt/β-catenin signalling pathway in mice brain (Shi et al., 2020). If Wnt/β-catenin signalling pathway is suppressed, BACE transcription is activated, followed by excessive proteolysis of APP and Aβ accumulation (Tapia-Rojas et al., 2016).

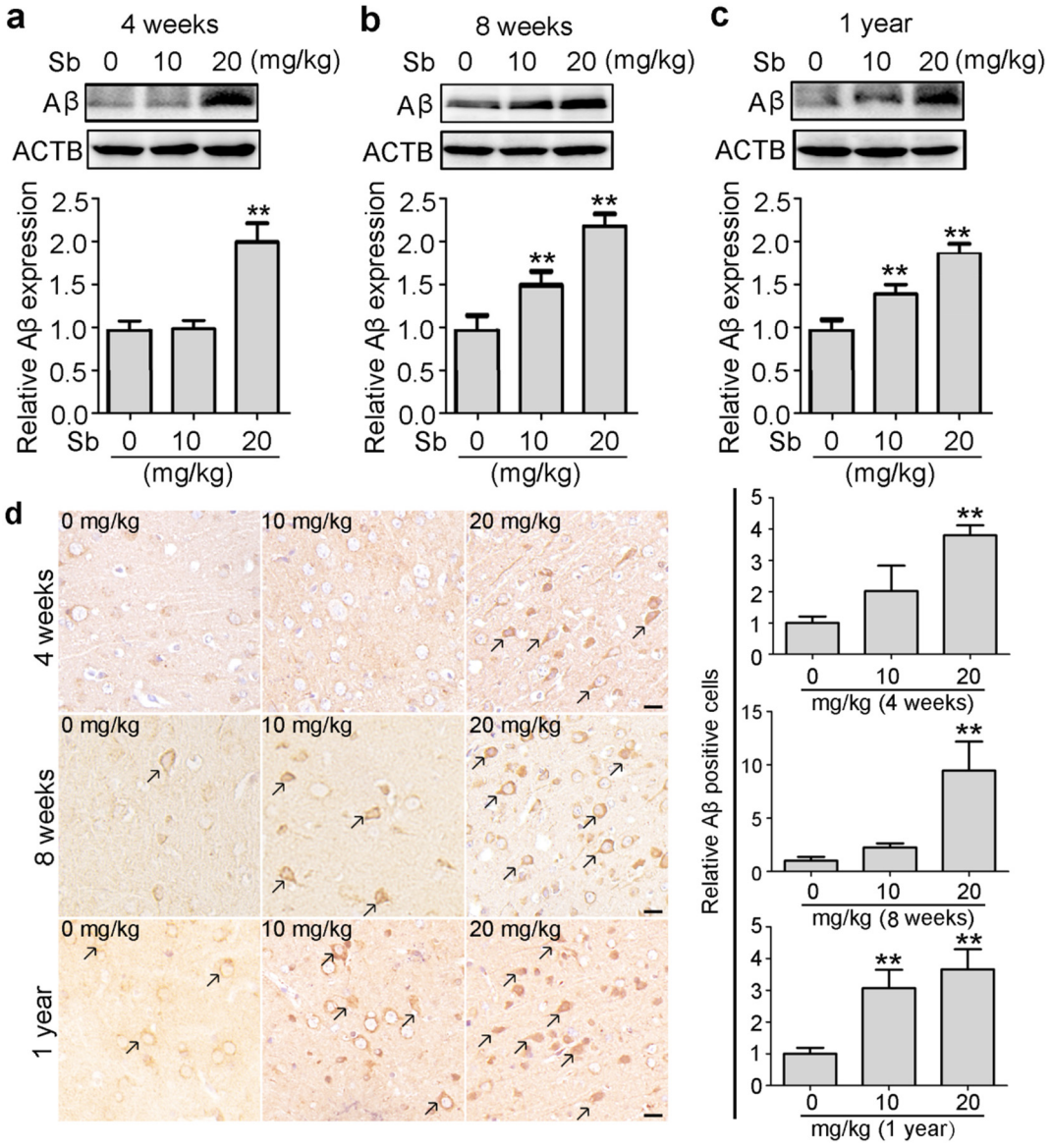

Fig. 2. The effects of antimony exposure on Aβ accumulation at the mice brain. (a–c) Western blot detection of Aβ expression levels in mice brain tissues exposed to Sb at indicated concentrations for 4 weeks (a), 8 weeks (b) and 1 year (c), respectively. The graph below shows the statistical analysis of the expression levels of Aβ compared with the control. n = 5. (d) IHC detection of Aβ expression levels in brain tissues of antimony-treated mice under indicated conditions. The graph right shows the statistical analysis of the relative Aβ positive cells compared with the control. All quantitative data are presented as mean ± SD. n = 3. Black arrows indicate Aβ expression positive cells. $^{**}p < 0.01$. Scale bar: 20 μm.

Also, autophagy is involved in AD development, Aβ production, and intracellular Aβ metabolism (Uddin et al., 2018). It is involved in Sb-triggered toxicity (Zhao et al., 2017). In autophagic-deficient APP transgenic mice, the Aβ levels were significantly reduced and Aβ secretion was reduced by 90% compared to controls, while Atg7 supplementation rescued Aβ secretion, suggesting autophagy is necessary for Aβ accumulation (Nilsson and Saido, 2014). Consistently, we found that Sb induced autophagy and neuronal apoptosis in brain (Wang et al., 2019). We will further explore the role played by GSK3β activation and autophagy caused by Sb exposure in the context of AD initiation and development. In addition, amyloid plaque formation is largely attributable to a reduced Aβ clearance rate (Kress et al., 2014). Apolipoprotein E (APOE), especially APOE 4, plays an important role in above clearance (Kloske and Wilcock, 2020). As mice aging, mitochondrial dysfunction becomes more severe; older mice cleared Aβ 40% less effectively than did younger mice (Volloch et al., 2020). We indeed found that the Aβ levels in control mice were increased with increased age.

We found that Sb at 20 mg/kg for 4 weeks stimulated Aβ accumulation, but failed to increase tau phosphorylation at ser396 and ser199, suggesting that Aβ accumulation precedes tau phosphorylation. Excessive tau phosphorylation compromises microtubule stability, induces synaptic dysfunction, and affects both protein degradation and autophagy (Alonso Adel et al., 2004; Dickey et al., 2007; Hoover et al., 2010). Tau has many phosphorylation sites with different functions, and may sometimes protect neurons. Hyperphosphorylation at certain sites triggers tau self-assembly into NFTs. For example, high-level phosphorylation of ser199 renders tau toxic; ser396 phosphorylation may change the isoelectric point, increase molecular interactions, and promote tau self-assembly (Alonso et al., 2018; Yu et al., 2019). We found that both ser199 and ser396 phosphorylation were upregulated by Sb. GSK3β and cyclin-dependent kinase 5 (CDK5) directly phosphorylate tau (Wilkaniec et al., 2016). Therefore, Sb-mediated GSK3β activation might contribute to tau hyperphosphorylation. CDK5 is specifically expressed in neurons and plays roles in AD initiation and development. p35 constitutively activates CDK5 to protect the central nervous system. Once stimulated, CDK5 binds to p25 to induce tau hyperphosphorylation. Possible upstream mechanisms underlying Sb-mediated tau hyperphosphorylation needed to be investigated.

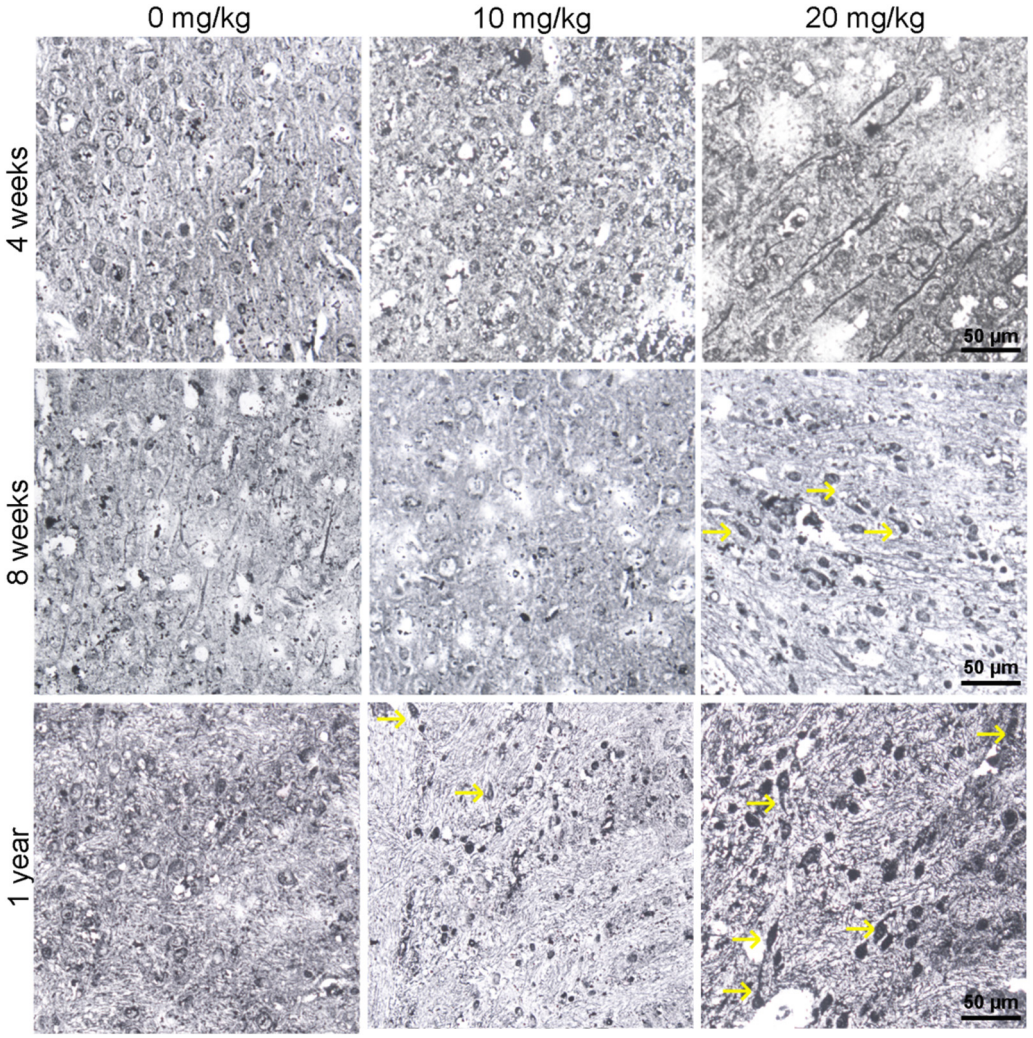

Fig. 3. Bielschowsky staining image of mouse brain exposed to antimony at different doses (0, 10, 20 mg/kg) for 4 weeks, 8 weeks and 1 year. Yellow arrows indicate NFT. Scale bar: 50 μm. n = 3.

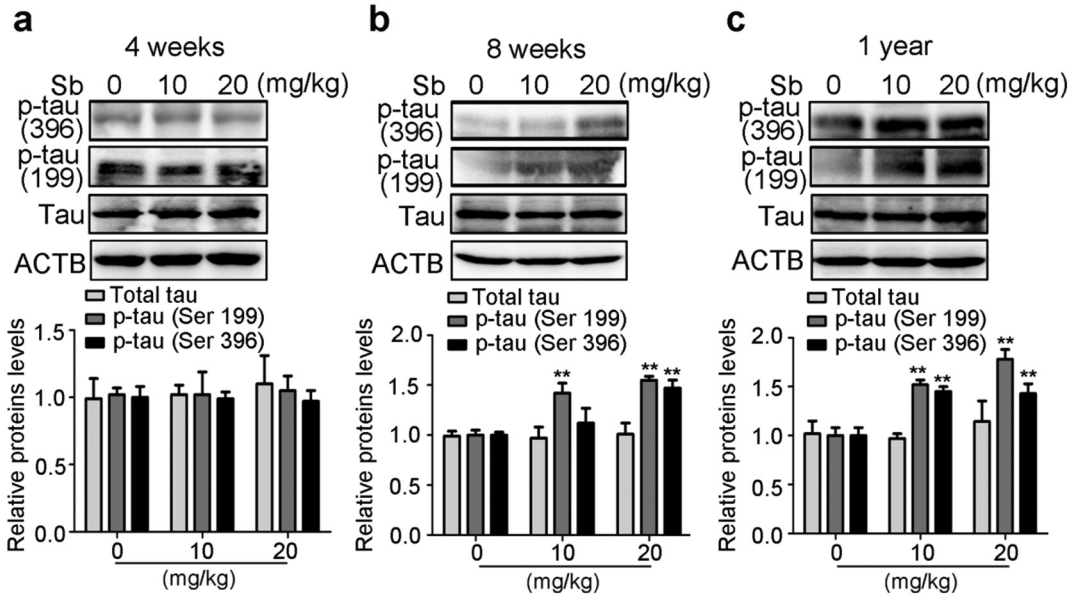

Fig. 4. The effects of Sb exposure on the phosphorylation levels of Tau protein at Ser 199 and Ser 396 sites in the mice brain. (a–c) Western blot detection of Tau, p-tau (Ser 199), p-tau (Ser396) expression levels in mice brain tissues exposed to Sb at indicated concentrations for 4 weeks (a), 8 weeks (b) and 1 year (c), respectively. The graph below shows the statistical analysis of the expression levels of Aβ compared with the control. n = 5. The graph below shows statistical analysis of the expression levels of each protein compared to the control. All quantitative data are presented as mean ± SD. $^{**}p < 0.01$.

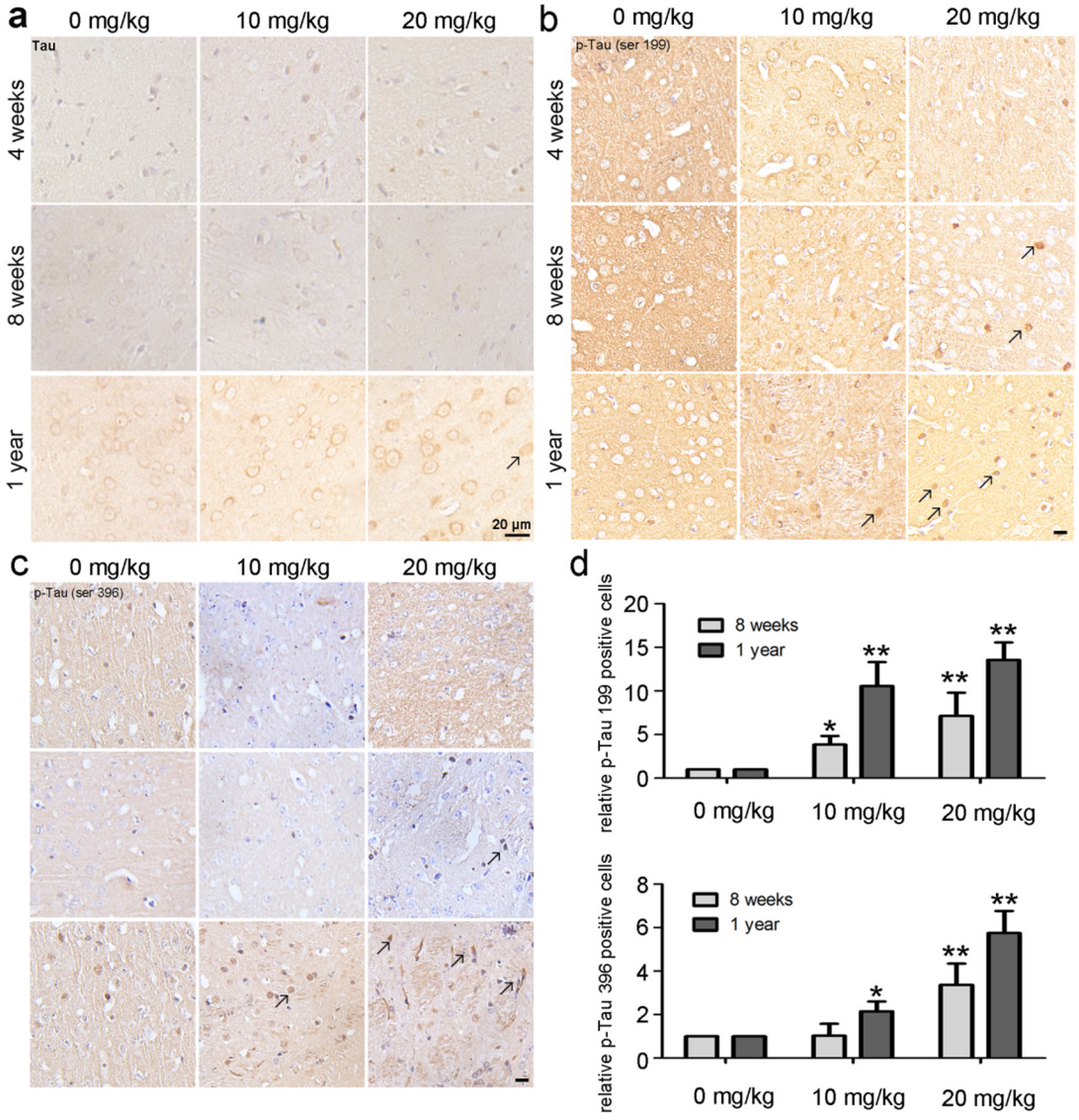

Fig. 5. Immunohistochemical detection of tau, p-tau (Ser 199) as well as p-tau (Ser 396). (a) The expression of tau protein in the mice brain exposed to different doses of antimony for 4 weeks, 8 weeks, and 1 year. (b) Expression of p-tau (Ser 199) in the mice brains of mice exposed to different doses of antimony for 4 weeks, 8 weeks, and 1 year. (c) Expression of p-tau (Ser 396) in the mice brains exposed to antimony at different doses for 4 weeks, 8 weeks, and 1 year. (d) The graph right shows the statistical analysis of the relative p-Tau ser 199 or 396 positive cells compared with the control. Black arrows indicate positive staining. Scale bar: 50 μm. n = 3.

In conclusion, we found that Sb promoted AD-like pathological changes. The results deepen our understanding of Sb toxicity and reveal a new AD risk factor. We plan to further explore detail mechanisms of Sb-induced AD pathogenesis.

CRediT authorship contribution statement

Shenya Xu: Investigation, Writing - original draft. **Zeyun Yang:** Investigation. **Ye Zhi:** Investigation. **Shali Yu:** Investigation. **Tao Zhang:** Investigation. **Junkang Jiang:** Resources, Visualization. **Jun Tang:** Investigation. **Hongsen He:** Investigation. **Ming Lu:** Resources. **Xiaoke Wang:** Writing - review & editing, Visualization. **Qiyun Wu:** Writing - review & editing, Conceptualization. **Xinyuan Zhao:** Writing - original draft, Conceptualization.

Declaration of competing interest

The authors declare that they have no known competing financial interests or personal relationships that could have appeared to influence the work reported in this paper.

Acknowledgments

This work was supported by Nantong Jiangsu scientific research project (JC2019027, JC2019137); the National Natural Science Foundation of China (81703255); Qing Lan Project for Excellent Young Key Teachers of Colleges and Universities of Jiangsu Province (2020); Large Instruments Open Foundation of Nantong University (KFJN2054).

References

Alonso Adel, C., Mederlyova, A., Novak, M., Grundke-Iqbal, I., Iqbal, K., 2004. Promotion of hyperphosphorylation by frontotemporal dementia tau mutations. J. Biol. Chem. 279, 34873–34881.

Alonso, A.D., Cohen, L.S., Corbo, C., Morozova, V., Elldrissi, A., Phillips, G., et al., 2018. Hyperphosphorylation of tau associates with changes in its function beyond microtubule stability. Front. Cell. Neurosci. 12, 338.

Arbel-Ornath, M., Hudry, E., Boivin, J.R., Hashimoto, T., Takeda, S., Kuchibhotla, K.V., et al., 2017. Soluble oligomeric amyloid-beta induces calcium dyshomeostasis that precedes synapse loss in the living mouse brain. Mol. Neurodegener. 12, 27.

Ashok, A., Rai, N.K., Tripathi, S., Bandyopadhyay, S., 2015. Exposure to As-, Cd-, and Pb-mixture induces Abeta, amyloidogenic APP processing and cognitive impairments via oxidative stress-dependent neuroinflammation in young rats. Toxicol. Sci. 143, 64–80.

Blennow, K., de Leon, M.J., Zetterberg, H., 2006. Alzheimer's disease. Lancet 368, 387–403.
Cai, T., Che, H., Yao, T., Chen, Y., Huang, C., Zhang, W., et al., 2011. Manganese induces tau hyperphosphorylation through the activation of ERK MAPK pathway in PC12 cells. Toxicol. Sci. 119, 169–177.
Choi, H., Kim, H.J., Kim, J., Kim, S., Yang, J., Lee, W., et al., 2017. Increased acetylation of Peroxiredoxin1 by HDAC6 inhibition leads to recovery of Abeta-induced impaired axonal transport. Mol. Neurodegener. 12, 23.
Dickey, C.A., Kamal, A., Lundgren, K., Klosak, N., Bailey, R.M., Dunmore, J., et al., 2007. The high-affinity HSP90-CHIP complex recognizes and selectively degrades phosphorylated tau client proteins. J. Clin. Invest. 117, 648–658.
Dieter, M.P., Jameson, C.W., Elwell, M.R., Lodge, J.W., Hejtmancik, M., Grumbein, S.L., et al., 1991. Comparative toxicity and tissue distribution of antimony potassium tartrate in rats and mice dosed by drinking water or intraperitoneal injection. J. Toxicol. Environ. Health 34, 51–82.
Ehehalt, R., Keller, P., Haass, C., Thiele, C., Simons, K., 2003. Amyloidogenic processing of the Alzheimer beta-amyloid precursor protein depends on lipid rafts. J. Cell Biol. 160, 113–123.
Hock, A., Demmel, U., Schicha, H., Kasperek, K., Feinendegen, L.E., 1975. Trace element concentration in human brain. Activation analysis of cobalt, iron, rubidium, selenium, zinc, chromium, silver, cesium, antimony and scandium. Brain 98, 49–64.
Hoover, B.R., Reed, M.N., Su, J., Penrod, R.D., Kotilinek, L.A., Grant, M.K., et al., 2010. Tau mislocalization to dendritic spines mediates synaptic dysfunction independently of neurodegeneration. Neuron 68, 1067–1081.
Huat, T.J., Camats-Perna, J., Newcombe, E.A., Valmas, N., Kitazawa, M., Medeiros, R., 2019. Metal toxicity links to Alzheimer's disease and neuroinflammation. J. Mol. Biol. 431, 1843–1868.
Joshi, G., Chi, Y., Huang, Z., Wang, Y., 2014. Abeta-induced Golgi fragmentation in Alzheimer's disease enhances Abeta production. Proc. Natl. Acad. Sci. U. S. A. 111, E1230–E1239.
Kloske, C.M., Wilcock, D.M., 2020. The important interface between apolipoprotein E and neuroinflammation in Alzheimer's disease. Front. Immunol. 11, 754.
Kress, B.T., Iliff, J.J., Xia, M., Wang, M., Wei, H.S., Zeppenfeld, D., et al., 2014. Impairment of paravascular clearance pathways in the aging brain. Ann. Neurol. 76, 845–861.
Li, H., Liu, C.C., Zheng, H., Huang, T.Y., 2018. Amyloid, tau, pathogen infection and antimicrobial protection in Alzheimer's disease -conformist, nonconformist, and realistic prospects for AD pathogenesis. Transl. Neurodegener. 7, 34.
Liu, P.P., Xie, Y., Meng, X.Y., Kang, J.S., 2019. History and progress of hypotheses and clinical trials for Alzheimer's disease. Signal Transduct. Target Ther. 4, 29.
Long, X., Wang, X., Guo, X., He, M., 2020. A review of removal technology for antimony in aqueous solution. J. Environ. Sci. (China) 90, 189–204.
Min, J.Y., Min, K.B., 2016. Blood cadmium levels and Alzheimer's disease mortality risk in older US adults. Environ. Health 15, 69.
Nilsson, P., Saido, T.C., 2014. Dual roles for autophagy: degradation and secretion of Alzheimer's disease Abeta peptide. Bioessays 36, 570–578.
Oshima, E., Ishihara, T., Yokota, O., Nakashima-Yasuda, H., Nagao, S., Ikeda, C., et al., 2013. Accelerated tau aggregation, apoptosis and neurological dysfunction caused by chronic oral administration of aluminum in a mouse model of tauopathies. Brain Pathol. 23, 633–644.
Saerens, A., Ghosh, M., Verdonck, J., Godderis, L., 2019. Risk of cancer for workers exposed to antimony compounds: a systematic review. Int. J. Environ. Res. Public Health 16.
Selkoe, D.J., Hardy, J., 2016. The amyloid hypothesis of Alzheimer's disease at 25 years. EMBO Mol. Med. 8, 595–608.
Shi, W., Tang, Y., Zhi, Y., Li, Z., Yu, S., Jiang, J., et al., 2020. Akt inhibition-dependent down-regulation of the Wnt/β-catenin signaling pathway contributes to antimony-induced neurotoxicity. Sci. Total Environ. 140252.
Strittmatter, W.J., Saunders, A.M., Schmechel, D., Pericak-Vance, M., Enghild, J., Salvesen, G.S., et al., 1993. Apolipoprotein E: high-avidity binding to beta-amyloid and increased frequency of type 4 allele in late-onset familial Alzheimer disease. Proc. Natl. Acad. Sci. U. S. A. 90, 1977–1981.
Sundar, S., Chakravarty, J., 2010. Antimony toxicity. Int. J. Environ. Res. Public Health 7, 4267–4277.
Tanu, T., Anjum, A., Jahan, M., Nikkon, F., Hoque, M., Roy, A.K., et al., 2018. Antimony-induced neurobehavioral and biochemical perturbations in mice. Biol. Trace Elem. Res. 186, 199–207.
Tapia-Rojas, C., Burgos, P.V., Inestrosa, N.C., 2016. Inhibition of Wnt signaling induces amyloidogenic processing of amyloid precursor protein and the production and aggregation of Amyloid-beta (Abeta)42 peptides. J. Neurochem. 139, 1175–1191.
Uddin, M.S., Stachowiak, A., Mamun, A.A., Tzvetkov, N.T., Takeda, S., Atanasov, A.G., et al., 2018. Autophagy and Alzheimer's disease: from molecular mechanisms to therapeutic implications. Front. Aging Neurosci. 10, 04.
Volgyi, K., Juhasz, G., Kovacs, Z., Penke, B., 2015. Dysfunction of endoplasmic reticulum (ER) and mitochondria (MT) in Alzheimer's disease: the role of the ER-MT cross-talk. Curr. Alzheimer Res. 12, 655–672.
Volloch, V., Olsen, B., Rits, S., 2020. Alzheimer's disease is driven by intraneuronally retained beta-amyloid produced in the AD-specific, betaAPP-independent pathway: current perspective and experimental models for tomorrow. Ann. Integr. Mol. Med. 2, 90–114.
Wang, X., Zhu, P., Xu, S., Liu, Y., Jin, Y., Yu, S., et al., 2019. Antimony, a novel nerve poison, triggers neuronal autophagic death via reactive oxygen species-mediated inhibition of the protein kinase B/mammalian target of rapamycin pathway. Int. J. Biochem. Cell Biol. 114, 105561.
Wilkaniec, A., Czapski, G.A., Adamczyk, A., 2016. Cdk5 at crossroads of protein oligomerization in neurodegenerative diseases: facts and hypotheses. J. Neurochem. 136, 222–233.
Yu, C.C., Jiang, T., Yang, A.F., Du YJ, Wu M., Kong, L.H., 2019. Epigenetic modulation on tau phosphorylation in Alzheimer's disease. Neural Plast. 2019, 6856327.
Zhao, X., Xing, F., Cong, Y., Zhuang, Y., Han, M., Wu, Z., et al., 2017. Antimony trichloride induces a loss of cell viability via reactive oxygen species-dependent autophagy in A549 cells. Int. J. Biochem. Cell Biol. 93, 32–40.
Zhou, C.C., Gao, Z.Y., Wang, J., Wu, M.Q., Hu, S., Chen, F., et al., 2018. Lead exposure induces Alzheimers's disease (AD)-like pathology and disturbes cholesterol metabolism in the young rat brain. Toxicol. Lett. 296, 173–183.